

Monitoring of wastewater percolation in unsaturated sandy soil using geoelectrical measurements at Gabal el Asfar farm, northeast Cairo, Egypt

Khaled M. Said Gemail

Received: 3 December 2010 / Accepted: 28 July 2011 / Published online: 21 August 2011
© Springer-Verlag 2011

Abstract The use of wastewater for irrigation in sandy soil increases the pollution risk of the soil and may infiltrate to the shallow groundwater aquifer. In such environment, some important parameters need to be obtained for monitoring the wastewater in the unsaturated zone over the aquifer. These parameters include clay content, heterogeneities of the upper soils, depth to the aquifer and the variations of groundwater quality. In the present work, the efficiency of DC resistivity method in forms of 1-D and 2-D measurements was studied for wastewater monitoring in the Gabal el Asfar farm, northeast of Cairo, Egypt. Forty-one Schlumberger soundings (VES) were performed then followed by three pole-dipole 2-D profiles along some considered regions within the area. The resistivity measurements were integrated with the boreholes, hydrogeological and hydrochemical (surface and groundwater samples) information to draw a clear picture for the subsurface conditions. The obtained results were presented as cross sections and 3-D visualization to trace the clay intercalations within the unsaturated zone. In addition, a vulnerability map was created using the obtained results from 1-D Schlumberger survey and confirmed with the 2-D resistivity profiling. The obtained results have shown that the 2-D resistivity imaging technique is a powerful tool for

mapping the small-scale variability within the unsaturated zone and the wastewater infiltration. However, limitations of resistivity techniques were observed in the area with limited resistivity contrast such as thin clay layers with brackish water background. Under that condition, the measured pattern of resistivity distributions depends on the applied electrode array, electrode spacing and using the available geological information during the inversion process.

Keywords Wastewater · 2-D resistivity imaging · Aquifer vulnerability · Sandy soils · Groundwater monitoring

Introduction

In arid and semi-arid areas the domestic wastewater is considered as water resources for irrigation purposes. In the sandy soil, the utilizations of treated water or sewage effluent in agriculture activities should be managed within certain conditions to reduce the pollution risk and to safeguard public health. Wastewater usually contains undesirable constituents such as salts, traces of bacteria and high concentration of trace elements Cr, Fe, Mn, Pb, etc. Such conditions may have deleterious effects on soils and shallow groundwater aquifers where the surface pollutants infiltrate into porous subsoil and reach to the aquifer layer.

The Gabal el Asfar farm was established in the north-eastern side of Cairo (about 25 km from Cairo) since 1915 and covers an area of about 1,250 ha (Fig. 1). The farm is bounded by residential areas from the west to south and sandy desert from east to northeast. For many years, the farm has been irrigated with primary treated to raw sewage effluent through a network system of open drains, which cover the whole area. To overcome the problem of

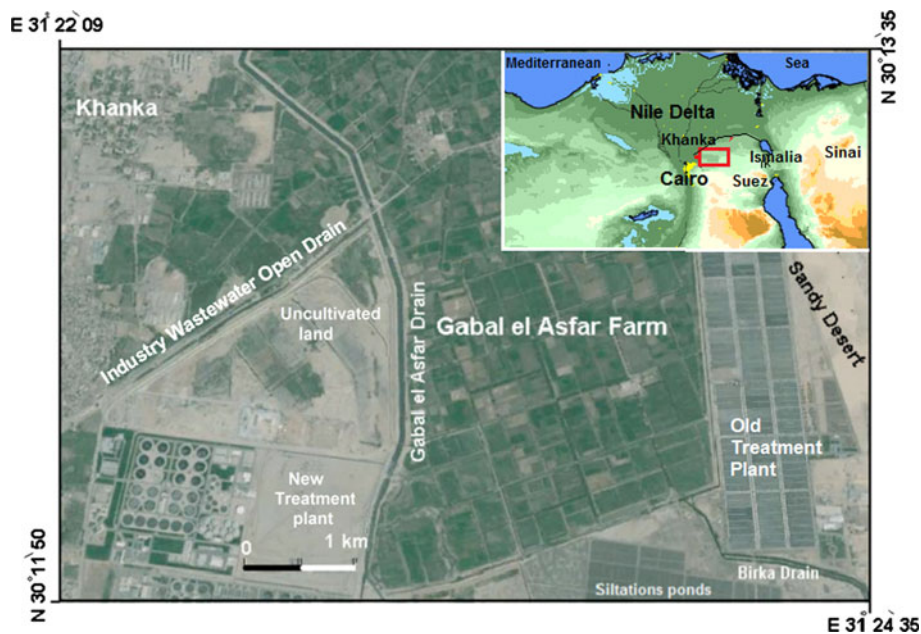
Electronic supplementary material The online version of this article (doi:10.1007/s12665-011-1283-6) contains supplementary material, which is available to authorized users.

Present Address:

K. M. Said Gemail (✉)
Department of Geology, Faculty of Science,
Zagazig University, Zagazig, Egypt
e-mail: kmg782@mail.usask.ca

K. M. Said Gemail
Geological Sciences Department, Saskatchewan University,
114 Science place, Saskatoon, SK S7N 2E5, Canada

Fig. 1 Location map of the Gabal el Asfar area, northeast Cairo



contamination, a treatment plant was recently constructed to treat the sewage water coming from north Cairo before its use. The treatment plant discharges the primary treated wastewater into Gabal el Asfar main drain then to Bilbeis drain in the north, which also receives wastewater from El Berka primary treatment plant and El Khossous wastewater lifting station in the south. The Gabal el Asfar main drain runs over sandy soils and collects the primarily treated and sometimes the raw sewage and industry wastewater (Fig. 2). Both sides of the main drain are cemented in parts while the bottom side is opened through graded sandy soil.

The farm area is underlain by the unconfined sand and gravel aquifer of Pleistocene, which belongs to the Nile Delta main aquifer (Rashed et al. 1995). About 40% of the water of Cairo is drawn from this aquifer which is located southeast of Nile Delta (Soliman et al. 1995). Under that condition, the presence of the open drains and using sewage for irrigation in sandy soil may represent a point source pollutant for the shallow aquifer. In this case, the presence of a clay cap can play an important role in the protection of the aquifer from the surface wastewater infiltrations. Therefore, it is very important to fully understand the detailed distribution and discontinuities of the clay aquitard in the area in order to study the vulnerability conditions of the aquifer with inhomogeneous cap (Sørensen Kurt et al. 2005).

The main goal of the present work is to study the applicability of resistivity method to provide information about the clay discontinuities and homogeneities of the soil above the aquifer in the area around the Gabal el Asfar drain and the farm. These discontinuities may act as pathways for the wastewater from the open drains to the shallow aquifer. To achieve this goal, DC resistivity measurements in the form of 1-D sounding and 2-D imaging profiling were carried out in

the area. For an effective use of resistivity techniques, the measurements were combined and integrated with available lithological, hydrogeological, and hydrochemistry data.

The determination of the spread of groundwater contaminations from wastewater is difficult because the cost of drilling and the rapid changes of subsurface layer distributions, which are common in the environmental investigations. Geo-electrical resistivity techniques provide the capability to map the lateral and vertical subsurface variations and monitoring of groundwater pollution in the areas between boreholes.

Resistivity measurements are commonly made at the ground surface using four point electrodes to detect variations in the bulk resistivity of the subsurface layers. However, in order to make further deductions concerning the subsurface conditions of the observed variations in resistivities some of the inherent ambiguity must be removed by making simplifying assumptions (Barker 1990). In the present work, a theoretical model is assumed based on the obtained geological and hydrogeological information from boreholes. This model was correlated with the observed resistivity profiles to draw a clear picture of the subsurface conditions in the whole area.

Geological and hydrogeological setting

The Gabal el Asfar farm represents a part of the Suez-Cairo Foothills desert area and covered by the Quaternary alluvial deposits. The eastern boundary of the area is characterized by higher elevation values than the western edge. The land surface has gentle slopes from 27 m above sea level at the eastern border to less than 15 m above sea level

Fig. 2 Images for wastewater discharge in the Gabal el Asfar area. **a** Gabal el Afar main drain running in sandy soil and collects different kind of wastewater. **b** Irrigation open canal cutting the cemented walls of the main drain. **c** Sandy soil with limestone boulders in the eastern bank of the main drain. **d** Industry and sewage water in the northwestern open drain. **e** Discharge of sewage and industry water into the main drain



at western and northwestern parts. The surface and groundwater flows are controlled mainly by the topographic gradient and porous sandy soil aquitard. Figure 3 is a simplified 3-D block, which shows the relationship between the surface topography and the flow patterns of surface and groundwater in the surveyed area. The surface wastewater and sewage are discharged from the western high land through a group of open drains towards the Gabal el Asfar main drain. Also, the main drain receives the primary treated wastewater from the new constructed treated plant in the southwestern corner. Towards the north, the both sides of the main drain are opened in sandy soil and receive a raw sewage and industry wastewater through some open drains (Fig. 2). These huge amounts of wastewater run to north direction towards the eastern Nile Delta fringe.

The upper soil in the area consists of graded sands with coarse grain texture. Abdel-Shafy and Abdel-Sabour (2006) studied the physical and chemical properties of the upper soil in the Gabal el Asfar farm with different irrigation periods using the wastewater. They concluded that the upper soil contains more than 75% of coarse grain sands. The clay particles vary between 0.04% in the uncultivated land and 20% in the cultivated lands which are irrigated for long period using sewage water. According to these conditions, a part of the sewage water used for

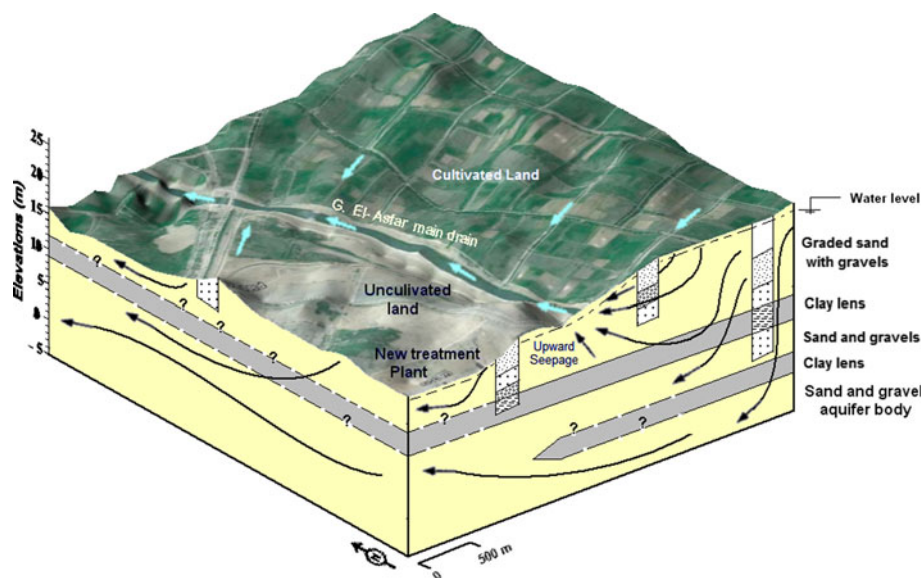
irrigation and from open drains seeps through the coarse sandy soil recharging the groundwater aquifer with contaminated water (Soliman et al. 1995).

Geologically, the Gabal el Asfar area is located west of the north–south fault, dividing the Quaternary sandy deposits on the west side and Miocene deposits in the east (Farid 1980). To the east, Holocene sand dunes locally cover the Pleistocene deposits before the Quaternary thins out and Miocene sands and limestone high lands are encountered (Aboel Abas 2001).

With respect to the hydrogeological setting of the area, the aquifer in the farm is an unconfined aquifer of Pleistocene age, which consists of graded sands and gravels with clay lenses. The thickness of this aquifer increases from 10 m in the southeast to greater than 65 m in northwestern corner (Rashed et al. 1995). The aquifer is recharged by sewage and primary treated wastewater from the southwestern lagoons and irrigation drain network, which are located at the high ground of the area. The total recharge rate was estimated by RIGW/IWACO (1991) as 0.5–2 m/year or about 50% of the total irrigation amount.

According to the available boreholes in the south boarder of the area, there are two clay intercalations which are found at 10–11 m above sea level and at about 2–5 m above sea levels (Rashed et al. 1995). In this case, the upper part of the aquifer is unconfined in the area, whereas

Fig. 3 Schematic block diagram shows the surface and groundwater flows in Gabal el Asfar area. The lithologic description modified after Rashed et al. (1996)



the clay lenses act as semi-confined conditions in the deeper part of the aquifer (Fig. 3). These clay intercalations in the upper part of the subsurface plays an important role for the infiltration speed of surface wastewater, which act as an impermeable barrier in the direction of the vertical water flow. Another important role for the clay accumulations at that level is the adsorption of heavy metals from the percolated sewage water (Aboel Abas 2001).

The regional flow in the deeper part of the aquifer is running from east to west. Piezometric levels are about 25 m above sea level in the east and about 15 m above sea level in the west (Fig. 3). The horizontal hydraulic conductivity of the aquifer ranges between 40 and 50 m/day and the transmissivity is about 5,000 m²/day (RIGW/IW-ACO 1991; Rashed et al. 1995).

To monitor the groundwater in the Gabal el Asfar farm, three surface water and three groundwater samples were collected from the northern part of the surveyed area. The surface water samples were collected from Gabal el Asfar main drain, primary treated irrigation water in the farm area (coming from El Berka primary treatment plant, southeast of the farm) and raw sewage water. Two groundwater samples were taken at different depths of 7 and 15 m from the northern part of the surveyed area along one profile perpendicular to the main drain and runs in the direction of water flow. The third groundwater sample was taken as reference point far away the surveyed area with 3 km in Khanka City. The chemical analyses of these samples are listed in Table 1. To monitor the groundwater variations during the last years, the chemical characteristics of the groundwater samples were compared with previous chemical analysis of Aboel Abas (2001) at the same water wells as shown in Table 1.

The chemical data showed a considerable decrease in the groundwater salinity at both wells as result of

percolation of irrigation water in the upper zone. At Khanka City (reference point) the groundwater salinity at shallow depth is about 2,200 mg/l indicating lateral variation in the groundwater within the urban area.

Geo-electrical measurements

The electrical resistivity surveys were collected using 1-D Schlumberger sounding and 2-D pole-dipole profiling in the farm and around the main drain of Gabal el Asfar area. The first survey was carried out by measuring 41 sounding points to cover the whole area (Fig. 4). These soundings were performed to provide information on the aquifer and aquitard distributions and to map the impermeable clays over the sandy aquifer. The measured soundings were distributed with unequal distance along four main profiles. The both sides of the main drain were covered by short distance points to detect the rapid changes around the drain. Schlumberger array was selected, with current electrode spacing ranging logarithmically from 1 to 300 m, depending on availability of space and geological data.

The measured sounding curves were processed and analyzed using IP2WIN program, in which the measured apparent resistivity and AB/2 values are inverted into true resistivities and thicknesses of the subsurface layers (Bobachev et al. 2003). This program is based mainly on linear filtering algorithm, which provides a fast and accurate direct problem solution for a wide range of models, covering all reasonable geological situations (Bobachev et al. 2003). During the inversion procedures, the principle of equivalence was taken into account where the same resistivity curve may produce many interpreted curves (Koefoed 1979; Van Overmeeren 1989). To select the model that best represents the true conditions of the

Table 1 Chemical analysis of surface and groundwater during the last ten years

	Surface water			Groundwater				
	Sw1 main drain	Sw2 irrigation canal	Sw3 raw sewage	Reference khanka	Aboel Abas (2001)		Present study	
					Gw1	Gw2	Gw1	Gw2
Depth (m)	0	0	0	8	7	10	7	10
TDS (mg/l)	730	460	750	2,100	1,079	1,285	720	892
Ec (mS/cm)	1.37	0.93	1.41	4.31			1.31	1.63
pH	5.71	5.95	6.8	6.93	6.9	6.9	5.74	5.82
Major elements (mg/l)								
K ⁺	18	15	18	23	30	22	20	19
Na ⁺	150	106	139	262	126	115	125	126
Ca ²⁺	70	68	115	198	134	170	114.4	120
Mg ²⁺	20.5	14.04	17	51.4	24	17	23.7	22
Cl ⁻	80	88	129	334	160	136	135	96
HCO ₃ ⁻	230.4	200.5	309	812	384	479	245	299
SO ₄ ²⁻	160	120	119	256	140	143	152	94
NO ₃ ⁻	16.2	19.8	50	55	117	202	93.3	167
Trace elements (mg/l)								
Al	0.056	<0.01	0.975 ^a	0.034			<0.01	<0.01
B	0.264	0.26		0.41			0.316	0.305
Cr	<0.003	<0.003	0.189	<0.003	<0.05	<0.05	0.005	<0.003
Cu	<0.003	<0.003	0.082	0.2	<0.05	<0.05	<0.003	<0.003
Fe ²⁺	<0.003	0.06	4.425	0.3	0.3	<0.1	<0.005	0.63
Mn ²⁺	0.06	0.04	0.249	0.5	0.2	<0.05	0.002	0.13
Ni	0.003	0.003	0.865	<0.01	<0.05	<0.05	<0.01	0.007
Pb	0.004	<0.003	0.146	<0.003	<0.05	<0.05	0.011	0.042
Zn ²⁺	0.013	0.153	0.245	0.2	<0.05	<0.05	0.243	0.5

^a The trace elements of the raw sewage water represent the mean average during the winter and summer seasons after Abdel-Shafy and Abdel-Sabour (2006)

subsurface, lithology and depths of subsurface layers were used to fix some layer parameters to obtain the actual resistivity values.

In addition to the Schlumberger sounding survey, three pole-dipole 2-D resistivity profiles were performed perpendicular to the main drain. The places of these profiles were selected according to the deduced results of 1-D sounding survey. The pole-dipole array was selected due to its high signal strength and has more penetration depths and good horizontal coverage compared with dipole–dipole or other arrays (Ward 1990). Along these profiles, data was acquired using three electrodes where the second current electrode was placed at 500 m from the measured profile. This distance is long enough to reduce the effect of the second current electrode (remote electrode). The acquisition instrument used was SAS 300C resistivitymeter, with electrode spacing 8 m and six investigation depth levels (*n*). These field parameters are enough to map the rapid changes within the top 20 m reaching to the upper part of the aquifer body.

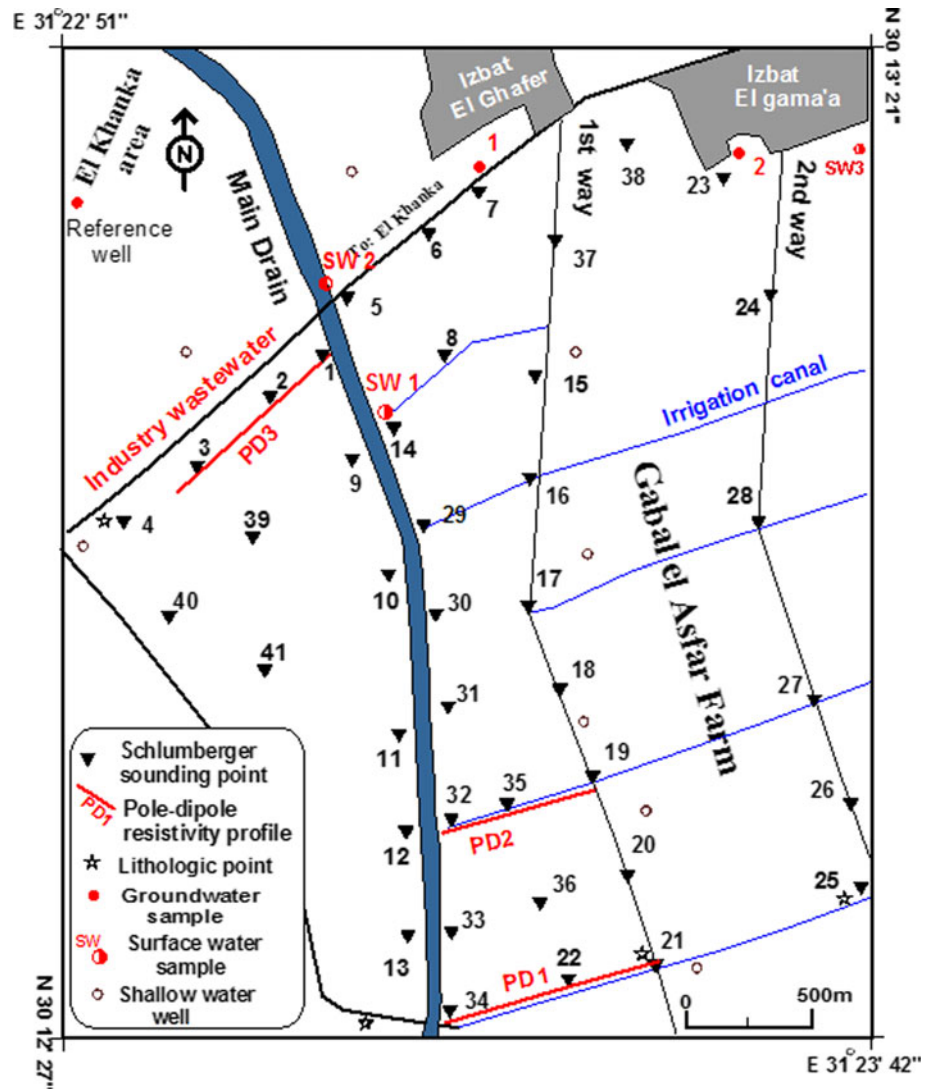
The measured 2-D resistivity profiles were processed and inverted with the smoothness-constrained least-square method (Loke and Barker 1996), by using the 2-D commercial software RES2DINV, Ver 3.4 for resistivity and IP interpretation (GEOTOM 2006). The inversion parameters were obtained by a 2-D synthetic model, which was created from the available geological information obtained from the boreholes in the southern border of the area.

Results and discussion

Schlumberger 1-D sounding

Based on the correlation between resistivity sounding results and the lithological information from the southern boreholes, three main resistivity layers are recognized in the area. The geo-electrical sections of Fig. 5 show the inverted resistivity distributions along two profiles run in east–west and north–south directions. Along these sections,

Fig. 4 Location map of the geo-electrical measurements and water samples



the unsaturated zone is represented by the first and second geo-electrical layers, which is composed of graded sands with local clay intercalations. This zone is partially saturated with wastewater percolated from the irrigation and sewage drain network. The wide range of resistivity within this zone is attributed to the high degree of heterogeneity as a result of variations of the grain size and water content, as well as the presence of some clay. The topmost zone, representing the subsoil, shows a resistivity range of 10–282 Ωm and thickness range of 1–5 m (Fig. 5). The variations of the surface soil resistivity are attributed to local conditions around the measuring soundings. The relatively higher values reflect dry sand and gravel soil that lies over the water table and far from the cultivated lands. The relatively lower resistivities indicate wet and fine sand, silt and clay soil as result of agricultural and irrigation activities.

The second geo-electrical layer, representing the protective layer above the saturated aquifer and corresponding

to clay lenses with relatively low resistivity range of 2–10 Ωm . The clay intercalations appear at 3 and 12 m depths as discontinued lenses with thickness range of 2–7 m. The thickness and the clay content of these intercalations are the dominating factors determining the infiltration speed of the surface wastewater in the farm area and around the main drain.

The third geo-electrical layer, representing the body of the aquifer in the area, exhibits two resistivity zones. The upper zone shows a resistivity range of 35–65 Ωm and the basal part has resistivity values between 12 and 35 Ωm , and decreases to <7 Ωm at great depths (soundings, 26, 27 and 2). The vertical variations in the aquifer resistivity are attributed to the salinity changes of the groundwater with depths. The upper part of the aquifer is recharged directly from wastewater (TDS, 420–730 mg/l) that used for irrigation for long period as well as the percolating water from the main drain and sewage open drains which are common in the area. The groundwater salinity in the basal part and

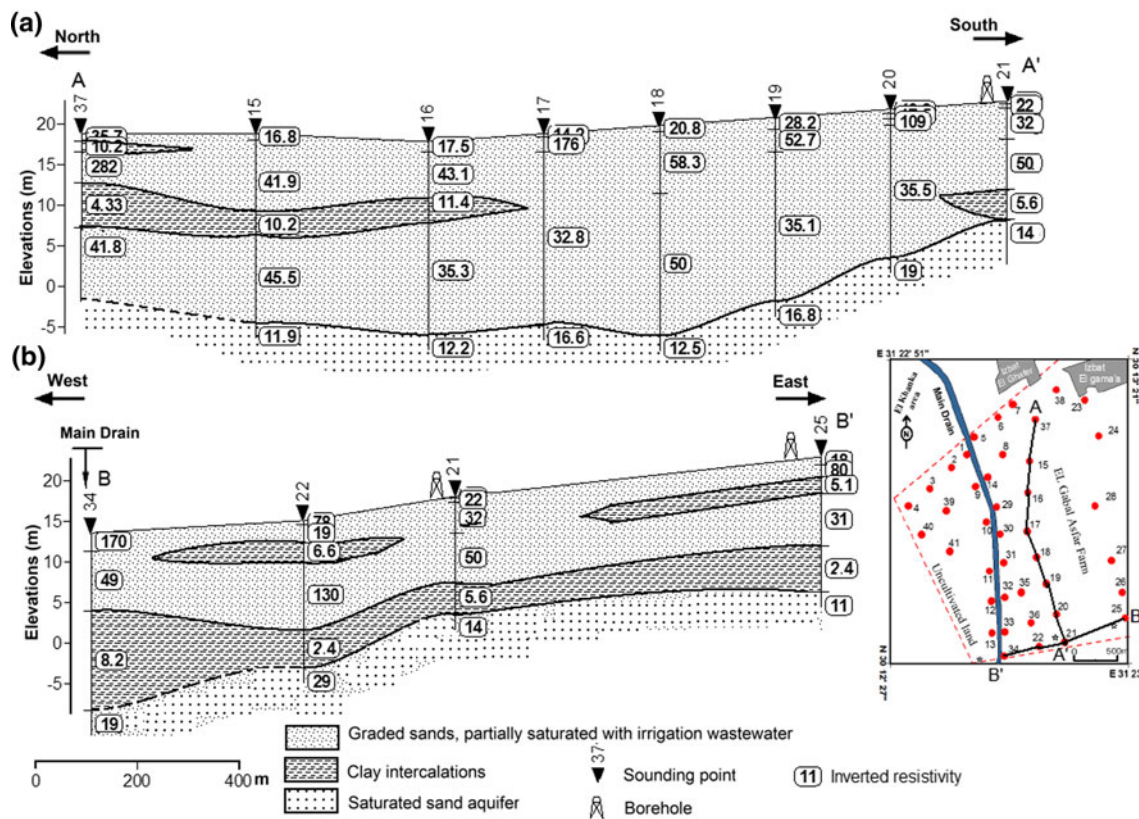


Fig. 5 Geo-electrical cross sections show the subsurface layer distributions in the area. **a** Profile A-A' running north–south in the middle part of the farm. **b** Profile B-B' running along the southern border of the area

in the uncultivated lands varies between 1,200 and 2,500 ppm (Rashed et al. 1995; Abdel-Shafy and Abdel-Sabour 2006).

To visualize the horizontal and vertical variations around the main drain and in the farm area, the interpreted resistivities with depths were used to create a 3-D model of the entire area. The output 3-D visualization model was computed using the inverse distance-anisotropic algorithm of the Rockworks software package (Rockware 2006). The anisotropic interpolation of thin beds such as clay intercalations allows mapping the geological sequence over many kilometers with sparse data observations (FitzGerald et al. 2009). The input data of this model was created by sampling of the true resistivities and depths of the subsurface layers at each measured sounding point. The sampling rate was low at shallow depths and increased with depth to explore the heterogeneities within the unsaturated zone. To produce a relatively fine mesh during the gridding process, the input gridding dimensions of 20, 20 and 2 m spacing (X, Y and Z, respectively) were applied. Figure 6 displays different views of the 3-D obtained model in the form of solid diagram, fence diagram of vertical sections and horizontal slices at different depths. To obtain a clear picture of surface layer distributions, the 3-D model was integrated with the available boreholes along the southern border.

The illustrations (Fig. 6) show a relatively high resistivity anomaly runs close to the main drain along the whole area where the both banks of the drain are cemented except its northwestern part, which receives a sewage and industry wastewater through an open sub-drain and characterized by low resistivity values (Fig. 2). This high resistivity zone extends to 4 m depth (Fig. 6d, slices 1 and 2) and corresponding to dry loose sands where the water level in the drain is about 3.75 m. In the area of soundings, 12, 32 and 35 (Fig. 6b and c) there is a local low resistivity zone crossing the main drain and may represent a leakage of the wastewater in the upper sand soil around the drain. The top soil in the eastern side of the surveyed area is characterized by relatively low resistivity values as a result of irrigation and agricultural activities.

On the depth zone of 5–15 m below the ground surface, very low resistivity zones ($>10 \Omega\text{m}$) appear in the southern and northern parts and totally disappear in the middle parts from east to west as shown in the vertical sections (Fig. 6b and c) and the horizontal slices (Fig. 6d, slices 2, 3 and 4). This zone is correlated with the clay intercalations over the aquifer layer which acts as protective layer in the southern and northern parts of the area. In the middle parts, the high resistivities values (35–60 Ωm) are caused by sandy inclusions in the clayey protective layer. The middle vertical

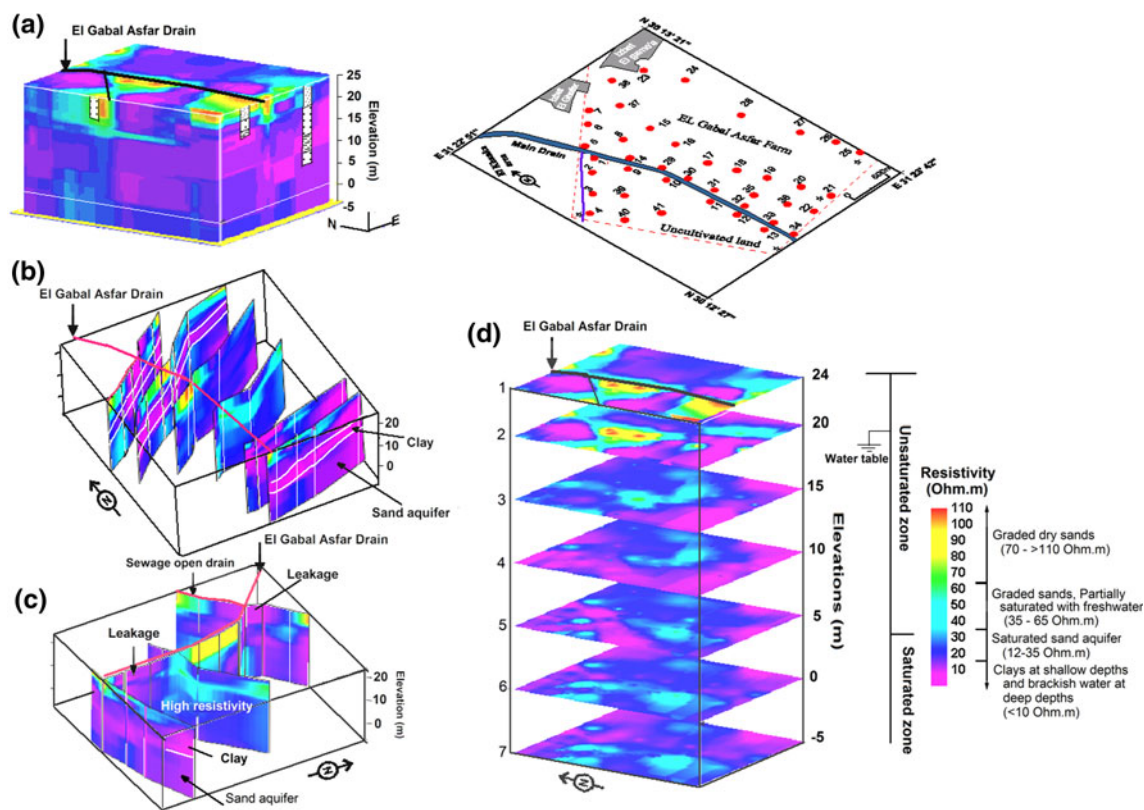


Fig. 6 3-D visualization resistivity model shows **a** solid diagram, **b** vertical cross sections perpendicular to the Gabal el Asfar main drain, **c** fence diagram around the main drain, **d** horizontal slices of resistivity at different depths

sections show that the aquifer layer is interconnected with the top soil by sandy deposits. Under those conditions, this sandy region is characterized by a high hydraulic connection and may act as windows for the sewage and wastewaters percolated from irrigation or from the main drain leakage and probably reach to the lower aquifer. The intensive sewage irrigation in the area leads to flushing and decreasing the salinity of the upper aquifer (Rashed et al. 1996; Aboul Abas 2001). The resistivity vertical distributions along the middle section (Fig. 6c) confirm the TDS pattern in the area where the middle parts are characterized by high resistivity values in comparison to the aquifer in the southern and northern sections. The clay lenses over the aquifer in the south are responsible for decreasing the vertical percolation of the low salinity irrigation water.

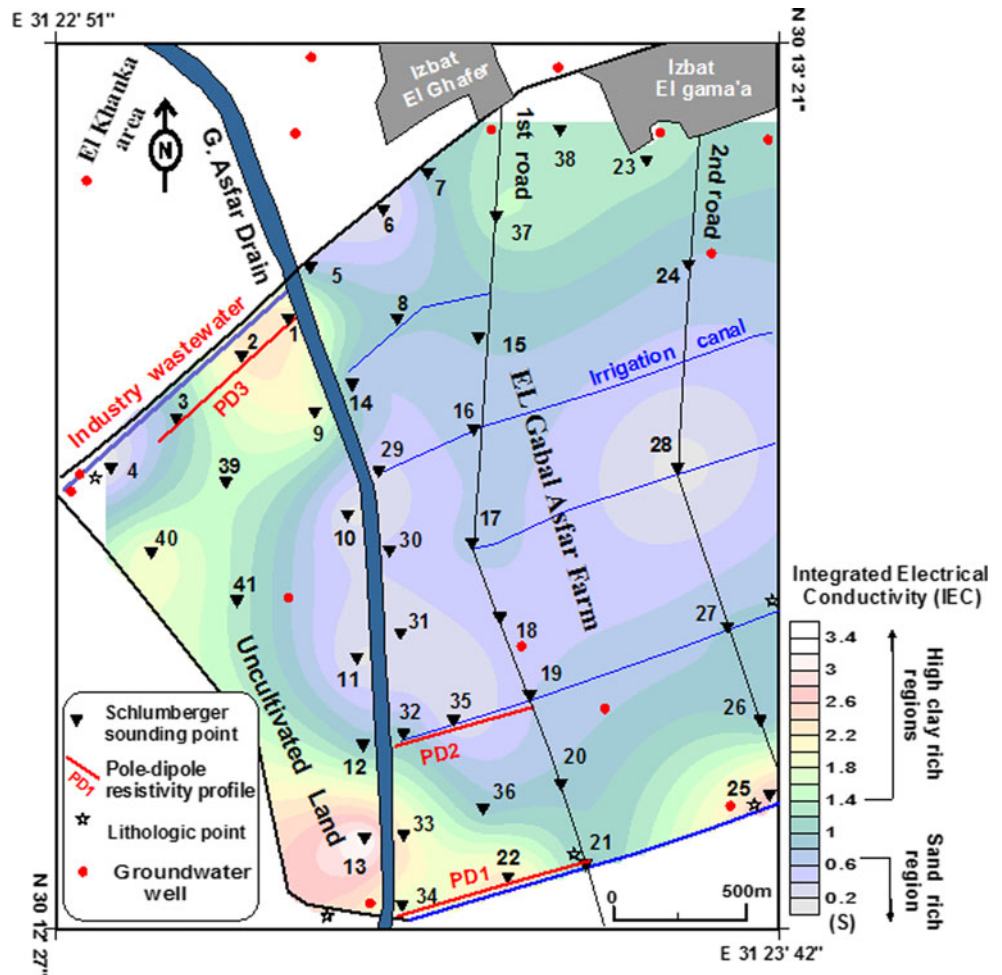
Assessment of aquifer vulnerability

The protection of the groundwater aquifer in the area is mainly controlled by the clay covering which are characterized by low permeability. The hydraulic resistance of the protective layer is based on the effective porosity for sandy materials and on the clay content for clay materials above the aquifer. Both parameters are controlling the electrical resistivity of the materials (Kirsch 2009). In this case, the

electrical conductivity (σ_i) or resistivity ($\rho_i = 1/\sigma_i$) is taking as equivalent to hydraulic conductivity (K_i) to calculate the hydraulic resistance (C) or aquifer vulnerability index, AVI ($C = \sum h_i/k_i$). According to Röttger et al. (2005), the calculated vulnerability index is called integrated electrical conductivity, IEC ($IEC = \sum h_i \times \sigma_i$). The estimated IEC unit is ohm^{-1} (Ω^{-1}) or siemens (S) (Casas et al. 2005).

To assess the aquifer vulnerability in the area, the interpreted resistivity (ρ_i) and thickness (h_i) of the geoelectrical layers above the aquifer were used to calculate of the IEC and can be used for quantification of aquifer vulnerability (Casas et al. 2008). Figure 7 shows the vulnerability map based on IEC for the Gabal el Asfar farm and the area around the main drain. This map displays a relatively low IEC values of less than 0.6 S in the middle region of the area and extends around the main drain. This low zone reflects the high vulnerability region (poor groundwater protection) that has a strong influence on the vertical infiltration capacity of surface wastewater as a result of the sandy rich soil. Clay rich soil can be easily distinguished on the southern region of the area, which is characterized by high IEC values (> 1 S). This region has a relatively good aquifer protection (low vulnerability) compared with the middle region where the presence of the clay rich soil reduces the vertical percolation of the surface

Fig. 7 Vulnerability map based on integrated electrical conductivity (IEC) for the Gabal el Asfar area



pollutants. In the northern region, there are some local low IEC spots referring low groundwater protection around the sewage open drain (Fig. 7).

The TDS, nitrate and heavy metals contents of the shallow groundwater exhibit a wide range of variability due to the rapid changes of the aquifer vulnerability (Rashed et al. 1996). In the area near sounding 18 in the middle high vulnerability zone, the groundwater has low salinity (900 mg/l) with high concentration of Fe and Mn. Within a short distance south of this point, the salinity raised to 1,879 mg/l at the same depths (Aboel Abas 2001). In the area east of the Gabal el Asfar drain chloride concentration in the upper part of the aquifer is stable, indicating substitution of the original groundwater by infiltrated irrigation water (RIGW/IWACO 1991; Rashed et al. 1996).

Resistivity imaging profiling

The resistivity imaging technique was applied perpendicular to the Gabal el Asfar main drain to image the surface leakage from the drain and the clay discontinuities around

the main drain. The three measured pole-dipole profiles run along three different vulnerability zones as indicated by the vulnerability map of the area (Fig. 7).

To check the accuracy of the method and its efficiency to locate the clay intercalations which act as barriers for the surface pollutants, a synthetic model was created using the same field parameters and compared with the obtained models of the three measured profiles. The available boreholes along the southern border of the area were used to produce the geological model as shown in the upper part of Fig. 8. The geological model simulates two clay intercalations in sand background. The upper clay layer has a 3 m thick and disconnected laterally at the middle part of the synthetic model. The second one rests on the upper part of the aquifer body and extends to 15 m depth with minimum thickness at its middle part. The resistivity ranges of the synthetic model were inferred from the former sounding survey and the parametric measurements near the boreholes along the southern border.

The synthetic modeling process was started by calculating the apparent resistivity distributions along the obtained geological model using the 2-D forward modeling

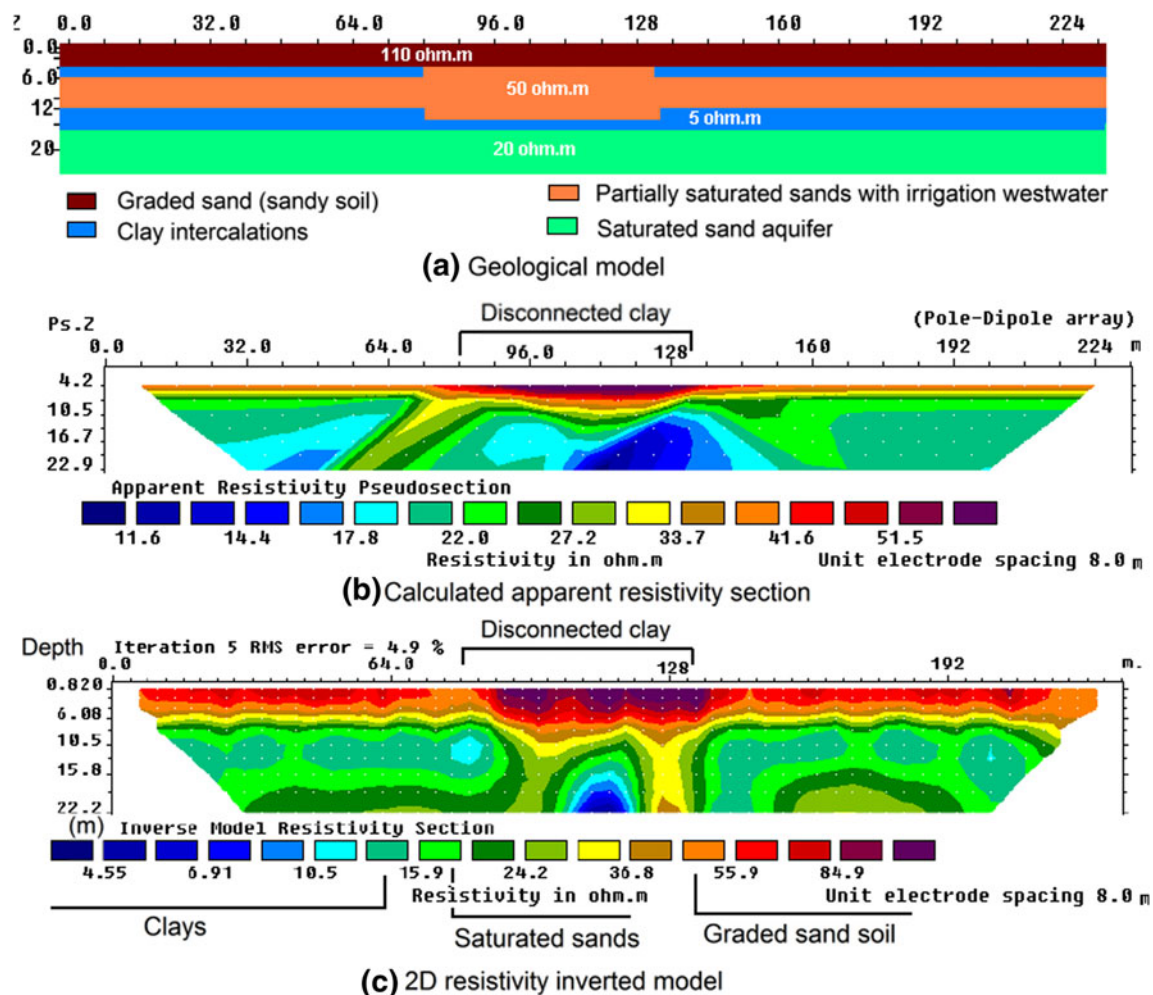


Fig. 8 2-D synthetic model using pole-dipole shows the resistivity patterns resulting from clay intercalations with sand background. **a** Geological model based on the boreholes in the southern border.

b Calculated apparent resistivities after adding 5% random noise. **c** Inverted 2-D resistivity section shows the resistivity distributions of the synthetic model

program, RES2DMOD (Loke 2002). The apparent resistivity calculations were carried out using finite-difference method and exported as data file with added 5% random noise. The calculated synthetic model was inverted using RES2DINV program to display the resistivity patterns resulting from the suggested geological model. During the inversion procedures, the inversion parameters were adjusted to image the suggested geological model. The final inversion parameters were saved in inversion parameter disk file and applied before the inversion process of the measured pole-dipole profiles.

Figure 8c shows the final 2-D inversion results of the synthetic model. The 2-D inverted model illustrates the progressive changes in the resistivity distribution patterns at the low clay content region (middle parts). The clay signature in the synthetic image can be seen as a low resistivity zone impressed within the partially saturated sands and shows a higher resistivity values of (15 Ω m) than the suggested values (5 Ω m). This problem is attributed to

the low thickness of the two clay intercalations compared with its depths and the background resistivities as well as the applied electrode spacing (8 m). However, the observed resistivity patterns are good enough to define the subsurface boundaries above the aquifer body and can be compared with the measured 2-D profiles.

Profile 1

The first pole-dipole profile (P1) runs along the southeastern boarder of the area. Figure 9a shows the 2-D inverted section of this profile. Along this profile, the image of resistivities against depth shows a general decrease in resistivity (from 250 to 9 Ω m) reflecting the vertical and lateral variations in the saturation degree and clay contents. As expected from the 2-D synthetic profile (Fig. 8), three layers structure can be noticed in the area close to the main drain. The first layer has a relatively high resistivities (90–250 Ω m) corresponds to dry graded sand

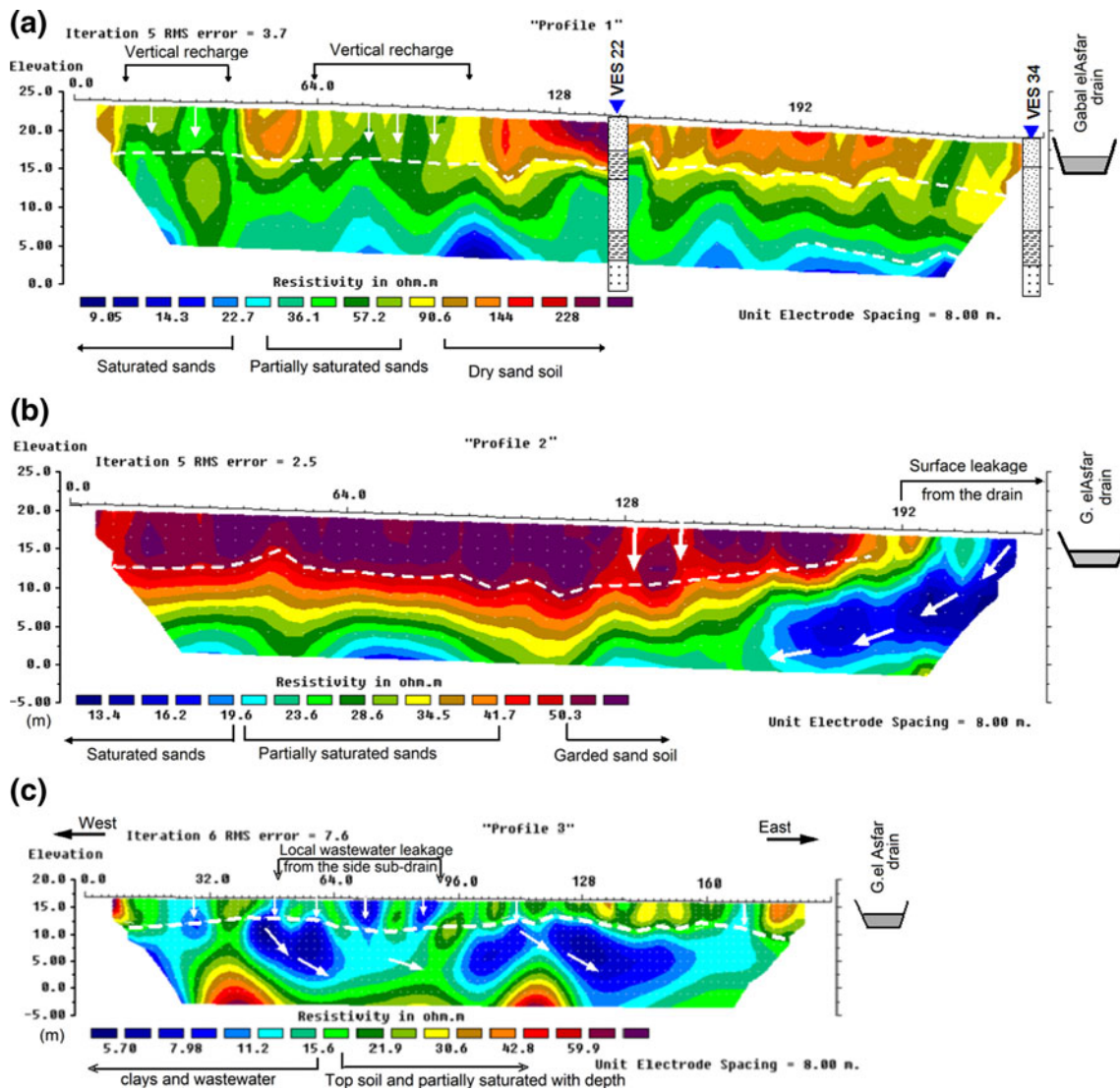


Fig. 9 2-D resistivity imaging sections using pole-dipole array. **a** Profile P1 along the southern border. **b** Profile P2 in the middle part of the area. **c** Profile P3 in the north-western border. The *dash line* is the boundary between the unsaturated sandy soil and saturated sand aquifer

(over the water table) and effective to depth of 8 m. Laterally, the resistivity distributions decrease within this layer towards east direction in the cultivated region as a result of infiltration of irrigation water. The second layer displays low resistivity values compared with the upper sandy soil indicating a partially saturated zone with irrigation water. The basal part of the inverted section represents the aquifer body in the area with low resistivities of 9 Ωm. These low resistivities are attributed to the lower clay intercalation which is marked the below aquifer layer as indicated from the boreholes and the former 1-D soundings. The effect of the upper clay intercalation appears as rapid vertical decreasing in the resistivity pattern in the area around VES 22 (Fig. 9a). As observed from the boreholes, the thickness of this intercalation is less than three meters and appears as local lenses. There is no clear connection between the

surface sandy soil and the aquifer body that can be noticed along this profile.

Profile 2

Figure 9b shows the inverted 2-D resistivity imaging profile obtained inside the eastern bank of the drain within the high vulnerability region which occupies the middle part of the Gabal el Asfar area. It can be clearly seen the low resistivity anomaly (13–20 Ωm) beside the drain which extends vertically from the surface sandy soil to the aquifer layer indicating a high saturation zone with wastewater. This region represents a leakage window for the surface wastewater from the drain to the aquifer layer. At that region, the both side of the drain are cemented to 4 m depth. However, the vertical percolation is coming from

the open bottom side of the drain as well as the microfissures in its cemented walls. The smoothly vertical variations of resistivity along the whole profile reflect the low clay content or totally absence of clay intercalations under the drain in this region. In this case, the resistivity distribution is controlled mainly by the degree of saturation and the groundwater salinity.

The layer distributions along this profile show low resistivity range (13–50 Ωm) compared with the first profile, P1 (Fig. 9a). The surface top sandy soil has higher resistivity values (42–50 Ωm) than the underlying partially saturated sands with resistivity range of 20–42 Ωm . A decrease of the resistivity in the upper soil can be noticed towards the main drain resulting from the lateral infiltration of irrigation water from the high eastern land as well as the leakage from the drain.

Profile 3

The third pole-dipole profile (P3) lies along the northwestern boarder of the area and runs parallel to the northwestern open sub-drain. This open drain runs on graded sandy soil with 4 m depth and discharges a raw industry and sewage wastewater towards Gabal el Asfar main drain (Fig. 2). This region is characterized by low and gentle topography compared with the southern and eastern region of the farm.

Figure 9c shows the inverted 2-D section for this profile. The comparison of this profile with the synthetic model (Fig. 8) and the other two profiles (P1 and P3) shows a great change in the resistivity distributions and subsurface conditions. It can be clearly seen the low resistivity values (<10 Ωm) in the upper parts of the inverted section (Fig. 9c), where the region is severely affected by infiltration of industry wastewater from the closed open sub-drain through the topmost sandy soil. The vertical infiltration in this region is affected by the low and gentle topography which acts to increase the infiltration in the upper parts where the surface water runs slowly in the top sandy soil. A significant decrease in resistivity values (5–10 Ωm) is noticed as local regions from 4 m depth downwards to 20 m. Such decreasing may be attributed to the salinity of groundwater, or the higher clay contents or both where the resistivity range is limited and there is no drilling evidence. A gradual increase of resistivity (16–43 Ωm) is observed towards the Gabal el Afar main drain resulting from an increase of freshwater leakage from the main drain where the salinity of disposal water in the drain is about 730 ppm at that place (water sample 1, Table 1). This may indicate the low sealing capacity of the main drain towards the north. The local low resistivity spots in the topmost soil can be interpreted as paths for the industry wastewater from the

closed open drain, which are connected with the subsoil partially saturated graded sands.

The heterogeneities of the soil along this profile confirm the obtained results of the vulnerability map (Fig. 7) and the 3-D model (Fig. 6) where the sandy soil in northern region of the area rapidly changes (lateral and vertical). These variations in subsurface conditions can be considered as the results of significant variability in clay content and the type and amount of the perched wastewater. The random pumping using shallow wells (hand pumps) and the open drains (the main drain also opens towards the north) increase the risk of wastewater percolation recharging the shallow perched aquifer in area and its surroundings.

Summary and conclusions

The discharge and reuse of sewage for irrigation of sandy soil represents the major sources of soil and groundwater pollution. In Egypt, sewage application takes place on sandy soil of the Gabal el Asfar farm through some open drainage ways. This area is covered by the Pleistocene graded sands and gravel, which represents the shallow aquifer in the area and its surroundings. This aquifer is marked by some clay intercalations with sand background. The accumulated clays in the upper soil (unsaturated zone) play an important role in the assessment of aquifer vulnerability for sewage water infiltration for two reasons. The great clay thickness over the aquifer layer reduces the infiltration speed of the wastewater, as well as adsorb of the heavy metals from the percolated water.

This paper was carried out to investigate the ability of resistivity method in the form of 1-D Schlumberger sounding and 2-D resistivity imaging techniques for characterization of groundwater protection in the Gabal el Asfar farm by mapping the lateral and vertical variations of the unsaturated zone over the aquifer body. This mapping process involved the heterogeneities of the clay intercalations and the permeable zones, which may act as vertical paths for the surface leakage of wastewater. From the inversion of resistivity data and hydrogeological as well as chemical analysis of shallow groundwater, the following conclusions are drawn:

- The response of the resistivity surveys (1 and 2-D) in the area is really satisfactory to monitor the percolated wastewater in the unsaturated zone. The 2-D resistivity sections show the powerful of 2D resistivity imaging technique for mapping the paths of surface wastewater leakage to the aquifer body. It has proved to be a useful and rapid tool for delineating the clay intercalations over the aquifer layer. In the case of thin clay layers, it is obvious that the applied electrode spacing of 8 m cannot

image the clay intercalations (<3 m thick), but it gives good evidence of the presence of anomalies in resistivity pattern as indicated from the synthetic modeling.

- The application of resistivity method (1 and 2-D) integrated by boreholes and water samples has demonstrated that the area of Gabal el Asfar farm is highly affected by using of sewage and primary treated wastewater for irrigation process. Part of the sewage water used for irrigation seeps through the upper sandy soil recharging the upper part of the Quaternary aquifer in the area. This part of the aquifer has been flushed (low salinity and high resistivity) more than its lower part and the surrounding groundwater.
- According to the constructed vulnerability map using resistivity data, the area could be differentiated into three regions with different hydrogeological and vulnerability conditions. The middle region has poor aquifer protection conditions compared with the southern region. The discontinuity of the clay bodies towards the middle region leads to increase the recharging rate of wastewater through the preamable sandy soil.
- The resistivity mapping outlines a large variation in the subsurface heterogeneity due to rapid variations of clay content, percolation of wastewater in the upper zone and groundwater salinity, which is influenced by the infiltrated irrigation water. In addition to providing information on the geological conditions, the 2-D resistivity sections around Gabal el Asfar main drain have outlined a local leakage from the drain towards the middle part of the area as result of low sealing capacity of the topmost soil.
- Although, the obtained results show the importance of resistivity surveys as monitoring tool to image the permeable pathways, a hydrogeological and environmental monitoring system should be continued especially in the middle part of the area where the aquifer body is directly connected with the surface through rich sandy soil.

Acknowledgments I wish to thank Fraïis Khadr and Mohamed Attwa, Zagazig University for their assistance during the field works. Also, I would like to thank Jim Merriam, professor of Geophysics at University of Saskatchewan, Canada for his careful review of the manuscript.

References

Abdel-Shafy H, Abdel-Sabour MF (2006) Wastewater reuse for irrigation on the desert sandy soil of Egypt: long-term effect. In: Hlavinec P et al (eds) Integrated urban water resources. Springer, Netherlands, pp 301–312

- Aboel Abas YM (2001) Rieselfelder Kairo: Verteilungsmuster anorganischer Schadstoffe in Boden und Grundwasser- Dissertation. Fakultät VI-Bauingenieurwesen und Angewandte Geowissenschaft, TU-Berlin. 183 pp
- Barker RD (1990) Investigation of groundwater salinity by geophysical methods. In: Ward S (ed) Geotechnical and environmental geophysics vol II. Investigation in geophysics, vol 5. Society of Exploration Geophysicist, Tulsa, pp 201–211
- Bobachev A, Modin I, Shevinin V (2003) IPI2Win V2.0: user's Guide. Moscow State University, Moscow
- Casas A, Himi M, Diaz Y, Pinto V, Font X, Tapias JC (2008) Assessing aquifer vulnerability to pollutants by electrical resistivity tomography (ERT) at a nitrate vulnerable zone in NE Spain. *Environ Geol* 54:515–520
- Farid S (1980) Nile delta groundwater study. M. Sc Thesis, Cairo University, Egypt, p 218
- FitzGerald D, Chilès J, Guillen A (2009) Delineate 3D iron ore geology and resource models using the potential field method. 11th SAGA biennial technical meeting and exhibition, Swaziland, 16–18 Sept 2009, pp 227–235
- GEOTOM (2006) RES2DINV software- user Manual. Accessed at <http://www.geoelectrical.com/download.html>
- Kirsch R (2009) Groundwater geophysics—a tool for hydrology. Springer, Heidelberg, pp 459–471
- Koefoed O (1979) Geosounding principles: resistivity sounding measurements, vol 1. Elsevier, Amsterdam, p 276
- Loke MH (2002) RES2DMOD version 3.01—Rapid 2D resistivity forward modeling using the finite-difference and finite element methods. Accessed at <http://www.geoelectrical.com/download.html>
- Loke MH, Barker RD (1996) Rapid least-squares inversion of apparent resistivity pseudosections by a Quasi-Newton method. *Geophys Prospect* 44:131–152
- Rashed M, Awad S, Salam MA, Smidt E (1995) Monitoring of groundwater in Gabal El Asfar wastewater irrigation area (Greater Cairo). *Water Sci Technol* 32(11):163–169
- RIGW/IWACO (1991) Development and mangement of Groundwater resources in the Nile Valley and Delta; Monitoring and control of groundwater pollution; Groundwater quality study Gabal el Asfar.-Research Institute for Groundwater, Ministry of Public works and Water Researches, El Kanater (internal Report), Cairo
- Rockware (2006) Rockworks 2008, user manual. Rockware Incorporated. Accessed at <http://www.rockware.com>
- Röttger B, Kirsch R, Scheer W, Thomsen S, Friberg R, Voss W (2005) Multifrequency airborne EM surveys—a tool for aquifer vulnerability mapping. In: Butler DK (ed) Near surface geophysics, investigations in geophysics, vol 13. Society of Exploration Geophysicists, Tulsa, pp 643–651
- Soliman MM, Nour El-Din M, Hassan NA (1995) Recharging of contaminated aquifer with reclaimed sewage water. *Environ Geol* 25:211–213
- Sørensen Kurt I, Auken E, Christensen N, Pellerin L (2005) An integrated approach for hydrogeophysical investigations: new technologies and a case history. In: Bulter Dwain K (ed) Near-surface geophysics. Society of Exploration Geophysicists, Tulsa, pp 585–597
- Van Overmeern RA (1989) Aquifer boundaries explored by geoelectrical measurements in the coastal plain of Yemen. A case of equivalence. *Geophysics* 54(1):313–324
- Ward SH (1990) Resistivity and induced polarization methods. In: Ward SH (ed) Geotechnical and environmental geophysics, vol 1. Society of exploration geophysicists, Tulsa, pp 147–190